STM JOURNALS

Journal of
Polymer & Composites

ISSN: 2321-2810 (Online)
ISSN: 2321-8525 (Print)
Volume 13, Special Issue 5, 2025
DOI (Journal): 10.37591/JoPC

https://journals.stmjournals.com/jopc

Research JoPC

Analysis of a Battery Pack Module for a Formula Student Car

Advait Jadhav[1], Shubh Dodia[2], Ved Chavan[3], Hari Vasudevan[4], Vinayak H. Khatawate[5,*]

Abstract

This research aims to evaluate the development of a high-voltage accumulator system that meets established standards of safety and operation. It examines key components, protocols, and techniques used in its creation while assessing performance in electronic cooling and structural integrity. Polymers, serving as electrical insulators and flame retarders, have found an interesting application in EV battery packs. This study focuses on polycarbonate materials' ability to withstand thermal and structural loads for safe battery operation and aims to exploit polycarbonate's high strength to weight ratio to function as cell holders. This test of modular assembly using polymers as an intermediate structural member helps to identify their potential applications in dynamical systems. The system includes the use of polycarbonate sheets for constructing the 64-cell battery pack module as part of an 8-segment setup, featuring 512 Molicel P42A Li-Ion cells with a capacity of 16.8Ah and a peak voltage of 537.6V. As there is a considerable loss of power to heat due to the high-voltage configuration, this study also explores forced air convection as a method for battery pack cooling, assessing its performance under normal operating conditions. The work guides battery pack design and cooling system optimization using Finite Element Methods, aligning with Formula Student 2023 regulations before vehicle integration.

Keywords: Electric vehicle, battery pack, thermal analysis, structural analysis, CFD, cooling, accumulator, finite element analysis

INTRODUCTION

Formula Student competitions are international events that challenge university students in dynamic and static events. The dynamic events include endurance, autocross, skid pad, and acceleration, while static events include design, cost & manufacturing, and business plan presentation. These competitions are sponsored by various companies and serve as a valuable recruitment channel. FSG (Formula Student Germany) is the main European competition and produces the main rules document implemented by other organizations such as Formula Bharat and Formula Student East.

ESF (Electrical Safety Form) and SES (Structural Equivalency Spreadsheet) validate designs from participating teams before scrutineering. The high-voltage accumulator is a vital component that powers the electrical tractive systems in the vehicle. DJS Racing Electric (DJSR) is an EV Formula Student from Mumbai, India. Having feats in combustion category, the team now aims to participate in their preliminary competitions in a fully electric category, with the elaborated accumulator and the EMRAX 228HV as their motor as a part of their powertrain package. Specifically, the DJSR E02 accumulator is composed of eight 64-

***Author for Correspondence**
Vinayak H. Khatawate

[1-3]UG student, Department of Mechanical Engineering, SVKM's Dwarkadas J. Sanghvi College of Engineering, Vile Parle, Mumbai, Maharashtra, India.
[4]Professor, Department of Mechanical Engineering, SVKM's Dwarkadas J. Sanghvi College of Engineering, Vile Parle, Mumbai, Maharashtra, India.
[5]Associate Professor, Department of Mechanical Engineering, SVKM's Dwarkadas J. Sanghvi College of Engineering, Vile Parle, Mumbai, Maharashtra, India.

Received Date: January 16, 2025
Accepted Date: April 08, 2025
Published Date: July 22, 2025

Citation: Advait Jadhav, Shubh Dodia, Ved Chavan, Hari Vasudevan, Vinayak H. Khatawate. Analysis of a Battery Pack Module for a Formula Student Car. Journal of Polymer & Composites. 2025; 13(Special Issue 5): S320–S339p.

cell modules that, when connected in series, can reach a maximum voltage of 537.6 V. This accumulator plays a crucial role in supplying power to both the Tractive System (TS) via DC-link and the Low Voltage (LV) system via DC/DC converter. It is important to note that the High Voltage (HV) and LV systems are separated by a voltage boundary of 60V DC [1]. Figure 1 provides a CAD-modelled image of the high-voltage accumulator comprising of the eight Segments of 64V each and its position concerning the Battery Management System. Figure 2 shows the employed cooling system. Figure 3 Shows the fan placement facilitating lateral airflow.

The objective of this work is to realize the effectiveness and purpose of the structural design of the polymer component and thermal optimization of the system, thereby validating the cooling system through CFD analysis concerning the following points:

- ***Temperature Control:*** Maintain Li-ion cell temperature below 55°C for improved efficiency as mentioned in the datasheet.
- ***Validate Staggered Arrangement:*** Evaluate the effectiveness of the inculcated staggered cell arrangement, considering packing efficiency, heat transfer, and overall performance.
- ***Apply Realistic Boundary Conditions:*** Establish inlet and outlet velocities mirroring real-world aerodynamics for enhanced accuracy in thermal analysis.
- ***Computational Model Robustness:*** Ensure the computational model's robustness using the k-epsilon turbulence model, balancing efficiency and precision.
- ***Inform Design Iterations**:* Generate data for iterative battery pack design, addressing thermal challenges and optimizing overall setup.

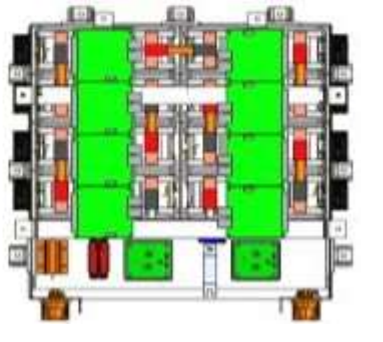	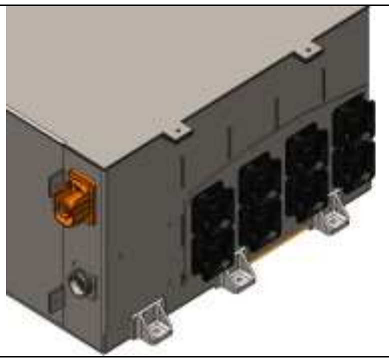	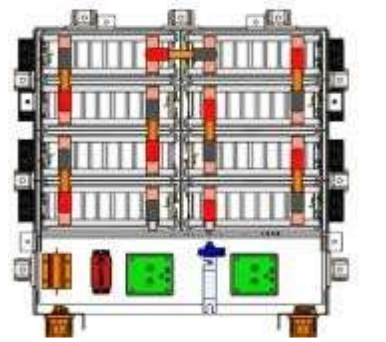
Figure 1. Top view of the system dividing the 8 modules of 64V each.	**Figure 2.** Cooling system.	**Figure 3.** Clearer segmentation of the modules underlying the Battery Management System

ACCUMULATOR SYSTEM DESIGN

Cell Selection

A comparative study of different cell types was done and a conclusion to employ cylindrical cells was arrived at. Cylindrical Cells have the following advantages over prismatic and pouch cells:

- Low cost per Wh.
- Better mechanical stability.
- High energy density.
- Better cooling efficiency due to gaps present upon close packing.
- Higher Capacity.
- Safe and reliable operation.

Molicel p42A with a better life and performance was selected for its high energy density, implying more capacity. Figure4 represents its manufacturer datasheet which gives valuable information of the cell discharge characteristics and optimal operating temperature. The Molicel series had several advantages:

- High thermal stability, high reliability

- Fast Charge
- Exceptional cycle life
- Very low impedance
- High Discharge current

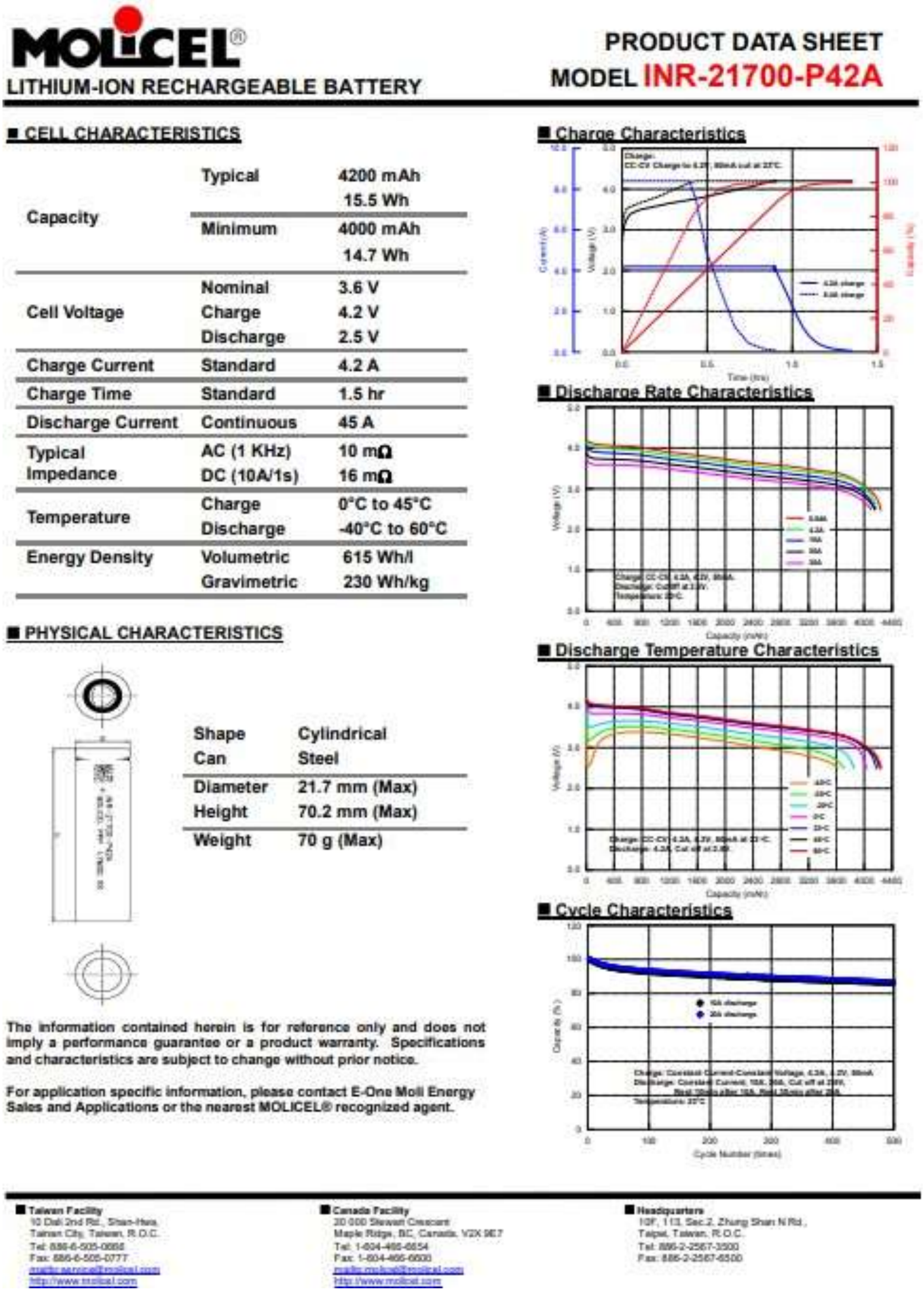

Figure 4. Product Datasheet for Molicel P42A Li-ion Cell [2].

Table 1 tabulates the overall specification of the battery pack and gives a total indication of the system's electrical output. It powers the EMRAX 228HV Motor and weighs over 85Kgs.

Battery Management System

The battery management system consists of a master-slave topology with 1 master and 8 slave PCBs (Printed Circuit Boards). Its main roles are to sense the voltage, current, and temperature to keep the cells within safe operating temperature. [3] The system ensures safe charging and discharging cycles and protection against shorting. The data obtained controls the thermal management system. The master-slave architecture offers easy debugging and less wiring. Using 10 NTC (Negative Temperature Coefficient) thermistors to cover 80% of the working cells [1], heat generated during operation is estimated and the data is used to control the thermal management system [4]. As shown in Figure 5, the slave assembly's modular lid-integrated construction allows easy access to the system for debugging and maintenance.

System efficiency and losses

Since the 512 Li-ion cells are electronically connected by Nickel and Copper busbars [4] as well as Radlok connections between segments, considering the following properties, the efficiency of the system has been estimated:

Busbar current calculation

Copper Busbar

Ampacity = 3.5 A/mm2

Area of cross section x Thickness x Ampacity = 14 x 2 x 3.5 = 98 A-mm

Nickel Busbar:

Ampacity = 1.5 A/mm2

Area of cross section x Thickness x Ampacity = 12 x 0.3 x 1.5 = 5.4 A-mm

Hence, approximating the system losses to 20% for safety purposes, considering both HV and LV Components to be generating heat during operation.

Table 1. Battery Pack overall specifications.

Maximum Voltage	537.6V
Nominal Voltage	460.8V
Maximum Charging Current	140A
Total Energy	3.65kWh
Total Number of Cells	512
Cell configuration	4p128s
Total Capacity	16.8Ah
Number of Cell Stacks<120V DC	8

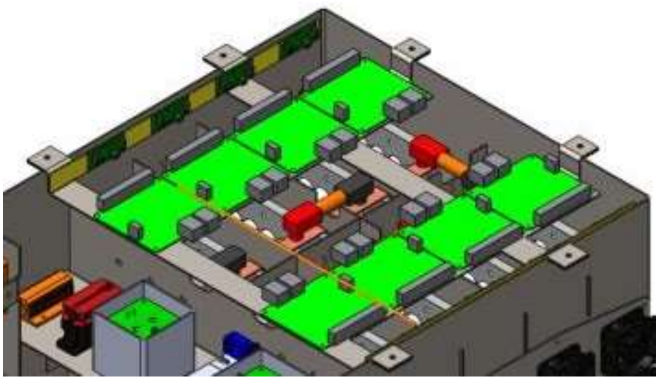

Figure 5. The slave assembly inside the accumulator.

CONSTRUCTION

Having the power limited to 80KW as per FSG Guidelines [1], the 512-cell battery pack is contained in AISI 1020 Steel with an epoxy powder coat. The internal walls dividing the modules are provided with slots to allow airflow. A modular lid sits atop the whole assembly covering both the accumulator top and front, allowing easy assembly or repair. The whole system is fabricated by laser cutting and Flux Wire Welding. The accumulator has nine Gussets which bear the weight as well as specified G-forces within the rulebook as it is mounted onto the chassis. A special plate to house the BMS (Battery Management System) is integrated with the lid's mounting points, and a separate integration of ACU (Accumulator Control Unit) components exists to avoid risky electrical failures as shown in Figure. 6. The entire assembly is covered with Nomex 410 paper [5].

Tractive System Accumulator Container (TSAC).

The TSAC is made of AISI 1020 Steel with due consideration of various factors and options. AISI 1020's high strength, better weldability and protection against the motor's electrical noise proved it to be our optimum choice. It has accommodation for the eight modules, ACU as well as the BMS and Cooling Fans. A hydrophobic mesh is used to guard against water intrusion.

Segment Design

A battery segment consists of 64 cylindrical Li-ion cells (Molicel P42A) packed between two polymer frames of Lexan 9034V polycarbonate. Figure 7. Shows how the constrainer strips are mounted over the frames using M3 bolts to keep the cells in place.

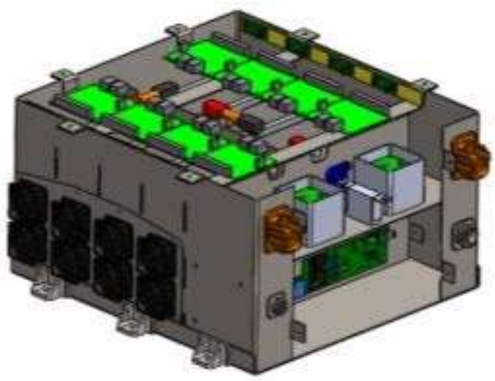

Figure 6. Isometric view of the accumulator.

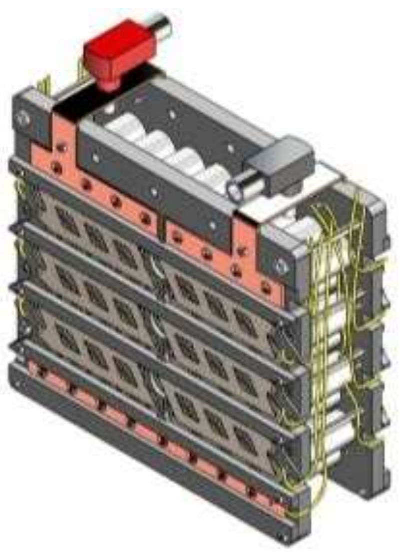

Figure 7. Isometric view of the 64-cell Module.

Laser-cut 2mm copper busbars are used to handle the current load, and nickel strips are spot-welded on the cells for connecting busbars. A top cover made of FR-ABS is mounted on top for insulation and fire retardancy. Voltage taps and thermistors are provided on the busbars for monitoring.

Frames

The Frames act as cell holders and they need to be both electrically insulating and flame retardant. In order to sustain the dynamic vibrations and g-forces from the vehicle's movement, they also demand a stable and strong assembly. Thus, the use of polymeric materials plays a unique role in providing insulation as well as structural integrity to the whole system. Polycarbonates being a tough, amorphous and transparent thermoplastic, serve as an ideal material for the battery pack assembly. With superior tensile & flexural strength, the Lexan 9034V is a flame-retardant, electrically insulating sheet used to construct the cell assembly [6,7]. The cells are sandwiched between the two 12mm Lexan Sheets milled with holes to accommodate the bolts as depicted in Figure 8. A 5mm Lexan piece is used as a part of the removable assembly which constrains the cells laterally while also easing disassembly in cases of failure. Slots are provided for wire routing and the frames weigh 170g each. Structural analysis of these frames is done taking the Lexan 9034V properties specified by the manufacturer as stated in Figure 9 [3,4,8].

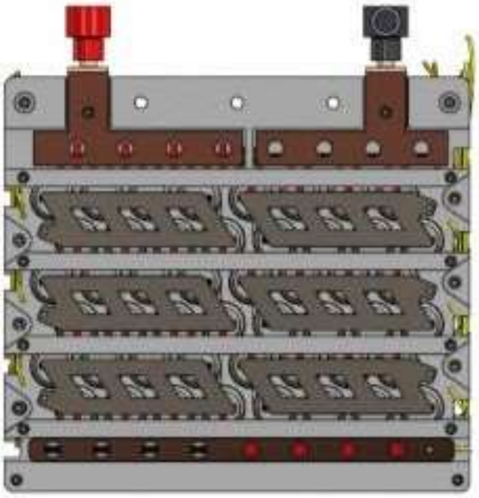

Figure 8. Front view of the module with constrainer strips and busbar connections.

PROPERTY	TEST METHOD	UNITS	VALUE 9034 *	9034V	9034HO
PHYSICAL					
Specific Gravity	ASTM D792	-	1.20	1.20	1.20
Refractive Index @ 77°F	ASTM D542A	-	1.586	1.586	1.586
Light Transmission (Average at 0.118")	ASTM D1003	%	86	86	86
Initial Haze		HU	<1	<1	<1
Rockwell Hardness (M scale)	ASTM D785	-	70	70	70
Rockwell Hardness (R scale)	ASTM D785		118	118	118
Taber @ 100 cycles	ASTM D1044				
	(ANSI Z26.1)	% haze	10	10	10
Water Absorption, 24 hrs	ASTM D570	%	0.15	0.15	0.15
Water Absorption, Equilibrium	@ 73°F	%	0.35	0.35	0.35
MECHANICAL					
Tensile Strength, Yield	ASTM D638	psi	9,500	9,500	9,500
Tensile Modulus	ASTM D638	psi	345,000	345,000	345,000
Flexural Strength	ASTM D790	psi	13,500	13,500	13,500
Flexural Modulus	ASTM D790	psi	345,000	345,000	345,000
Compressive Strength	ASTM D695	psi	12,500	12,500	12,500
Compressive Modulus	ASTM D695	psi	345,000	345,000	345,000
Poisson's Ratio	ASTM E132	-	0.37	0.37	0.37
Izod Impact Strength Notched @ 0.118"	ASTM D256A	ft-lbs/in	12–16	12–16	12–16
Unnotched @ 0.118"			60 (no failure)	60 (no failure)	60 (no failure)
Shear Strength @ Yield	ASTM D732	psi	6,000	6,000	6,000
Shear Modulus	ASTM D732	psi	114,000	114,000	114,000

ISSN: 2321-2810 (Online), ISSN: 2321-8525 (Print)

PROPERTY	TEST METHOD	UNITS	VALUE 9034 *	9034V	9034HO
THERMAL					
Coefficient of Thermal Expansion	ASTM D696	in/in/°F	3.75 x10 [illegible]	3.75 x10 [illegible]	3.75 x10 [illegible]
Coefficient of Thermal Conductivity	ASTM C177	Btu•in/hr•ft2•°F	1.35		1.35
Specific Heat @ 40°C	ASTM C351	BTU/lb-°F	0.30		0.30
Heat Deflection Temperature @ 264 psi	ASTM D648	°F	270	266	270
@ 66 psi			280		280
Brittle Temperature (on resin)	ASTM D746	°F	-211	-211	-211
FLAMMABILITY					
Horizontal Burn (Flame Spread) AEB	ASTM D635	in	<1		<1
Ignition Temperature, Self		°F	>1000	>1000	>1000
UL Flammability (File # 121562) Add link to	UL94HB	Pass/Fail	HB		HB
the UL site	UL94VO	Pass/Fail		≥0.236	
	UL94V2	Pass/Fail		≥0.060	
ELECTRICAL					
Dielectric Constant @ 60 Hz	ASTM D150	—	3.17		
Volume Resistivity	ASTM D257	Ohm-cm	8.2 x 1016		
Dissipation Factor (@60 Hz) also known as Power Factor	ASTM D150		0.0009		

Figure 9. Product datasheet for Lexan Polycarbonate 9034 [9].

STRUCTURAL ANALYSIS

The structural analysis focuses on stress generation and concentration in polycarbonate segment frames of the accumulator, using Finite Element Analysis (FEA). Boundary conditions, including vehicle acceleration and applied forces, are predetermined through simulations. The battery segment requires comprehensive structural analysis to validate the design. Segments must comply with the EV 5.5.8 rule in the FS 2024 rulebook [1] and withstand specific G-forces in longitudinal, lateral, and vertical directions. ANSYS Workbench Software is utilized for the FEA. Obtained results are shown from Figure 10 – Figure 18.

Material: Lexan Polycarbonate 9034

Applied Loads:

● **Acceleration:**
▪ Longitudinal: 40g
▪ Lateral: 40g
▪ Vertical:20g

● **Weight:**
▪ 1 cell: 70 grams
▪ 1 frame: 240 grams

A tetrahedral mesh with a 1mm size is selected since the frame has an intricate design that includes several holes for cells and restricting components [10-12]. Since the segment weight is 6.1 Kg and the force acting on the segment = Weight of Segment in Kg × 40g or 20g. Thus, for longitudinal and lateral directions, the force applied is 2400N, and for vertical direction, the force is 1200N. In all cases, three M6 bolting holes which are used to mount the segments onto the TSAC are kept as fixed support.

Structural Analysis Results

For structural validation, calculations were performed and the results obtained are as follows:

- *Internal Wall Weld Strength* Permissible Weld Strength = 90 MPa. Shear stress for 40g = 43.63 MPa. Shear stress for 20g = 21.81 MPa.
- *Slotted Internal Wall Weld Strength* Permissible Weld Strength = 90 MPa. Shear stress for 40g = 65.51 MPa. Shear stress for 20g = 32.76 MPa.
- *External Wall Weld Strength* Permissible Weld Strength = 90 MPa. Shear stress for 40g = 12.88 MPa. Shear stress for 20g = 6.44 MPa.

- *Bolt Strength for Segment Mounting* Permissible Tensile Strength = 940 MPa. Permissible Shear Stress = 470 MPa. Longitudinal Tensile Stress (40g) = 14.11 MPa.
- Lateral Shear Stress (40g) = 14.11 MPa. Vertical Shear Stress (20g) = 7.056 MPa.
- *Segment Weight Validation* The total weight of each segment is 6.03 kg as per EV 5.5.6 in FS Rulebook 2024 [1].

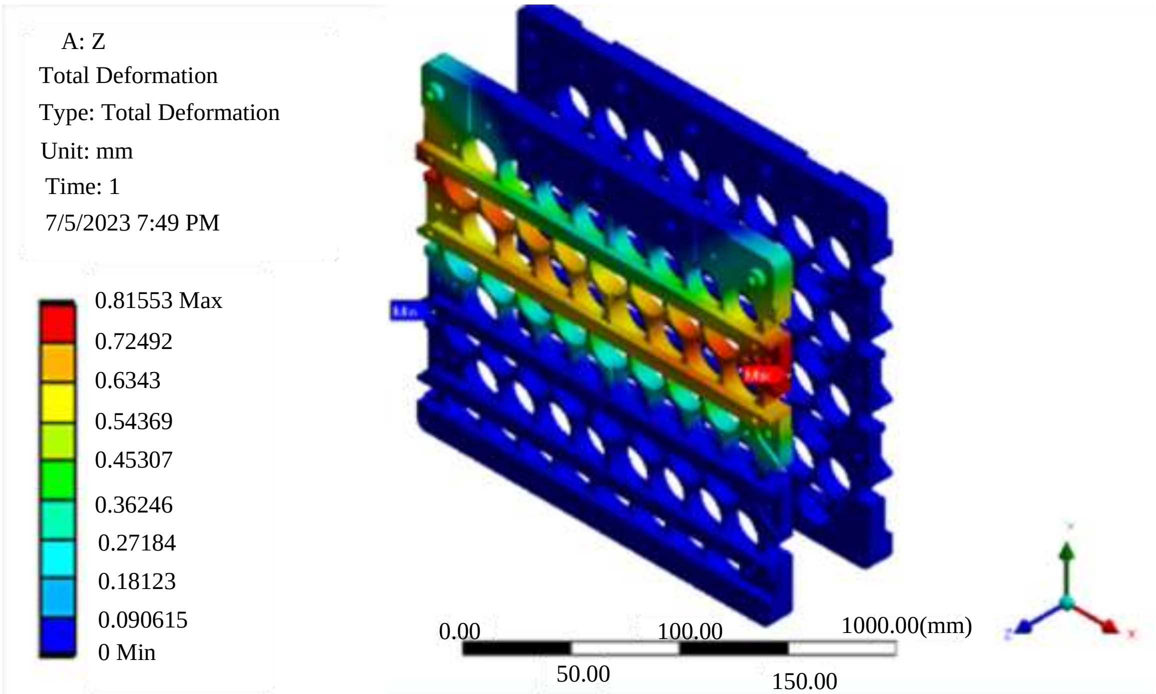

Figure 10. Total deformation of the frames when 40g is applied in the longitudinal direction.

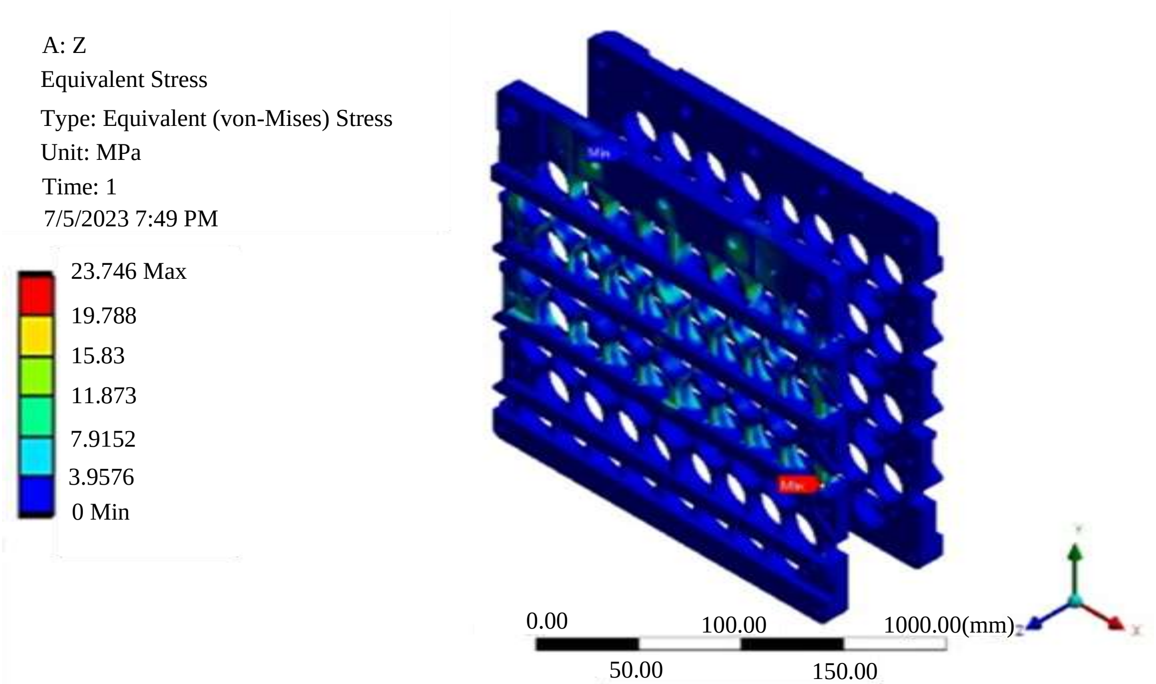

Figure 11. Equivalent Stress of the frames when 40g is applied in the longitudinal direction.

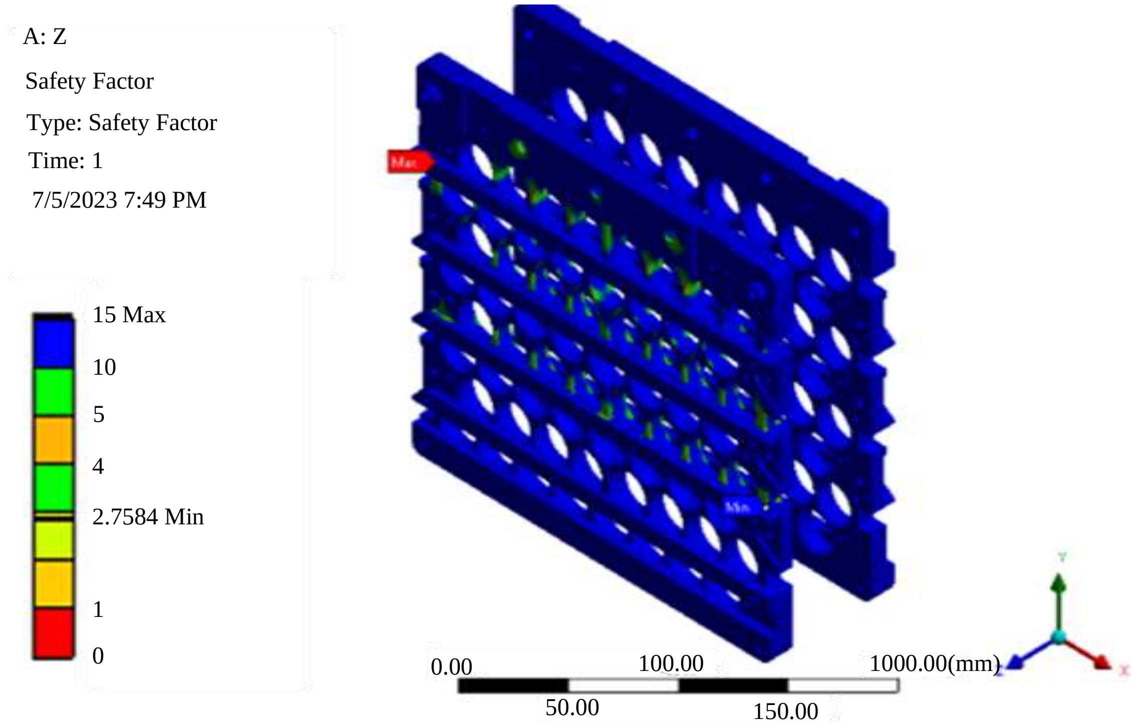

Figure 12. Factor of Safety for the frames when 40g is applied in the longitudinal direction.

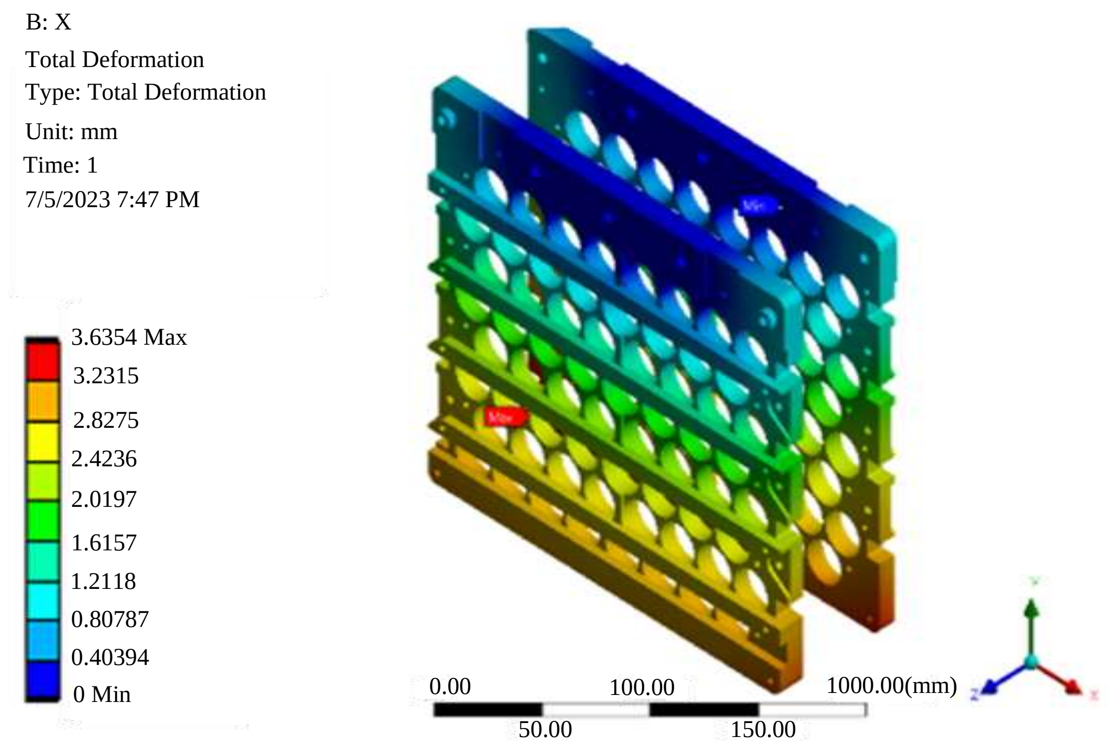

Figure 13. Total Deformation of the frames when 40g is applied in the lateral direction

The structural integrity of the assembly is well within prescribed limits and suitable for implementation in the FS Vehicle. FEA analysis using a 2mm tetrahedral mesh provided accurate and dependable results. Subsequent iterations also yielded the same results, and structural testing successfully met safety and mechanical design regulations, thus verifying the use of a flame-retardant polymer, having high strength to weight ratio in battery pack applications. Figure 19 elaborates the segment mounting mechanism to the container walls in a system of 3 Bolts. Figure 20 indicates the SES-compliant vent design to allow fan mounting and lateral airflow. Figure 21 gives an exploded definition of the segment module and illustrates its complete assembly.

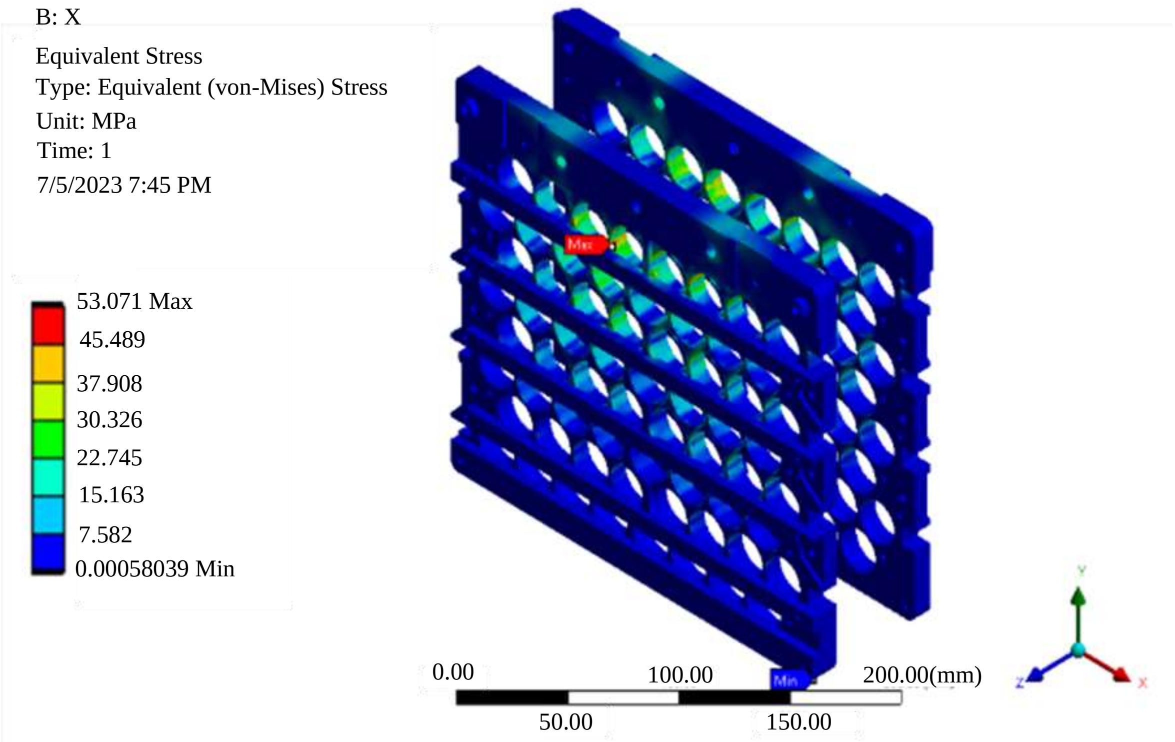

Figure 14. Equivalent Stress of the frames when 40g is applied in the lateral direction

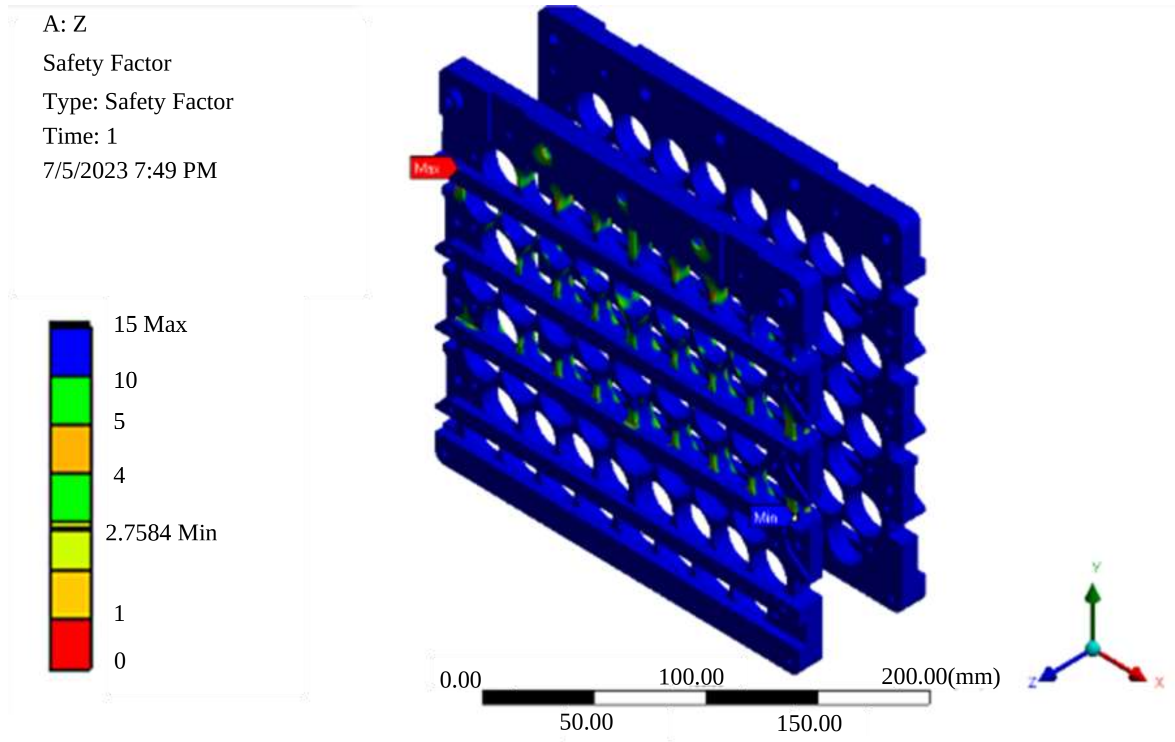

Figure 15. Factor of Safety for the frames when 40g is applied in the lateral direction

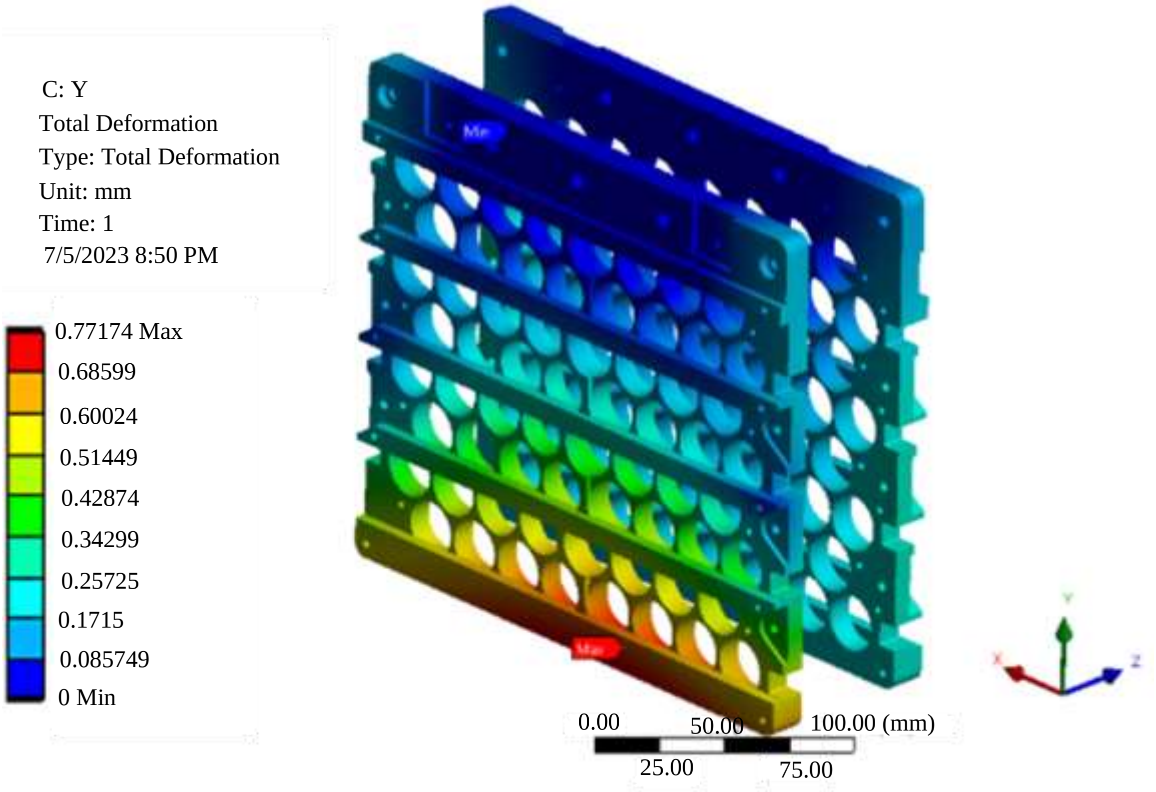

Figure 16. Total Deformation of the frames when 20g is applied in the vertical direction.

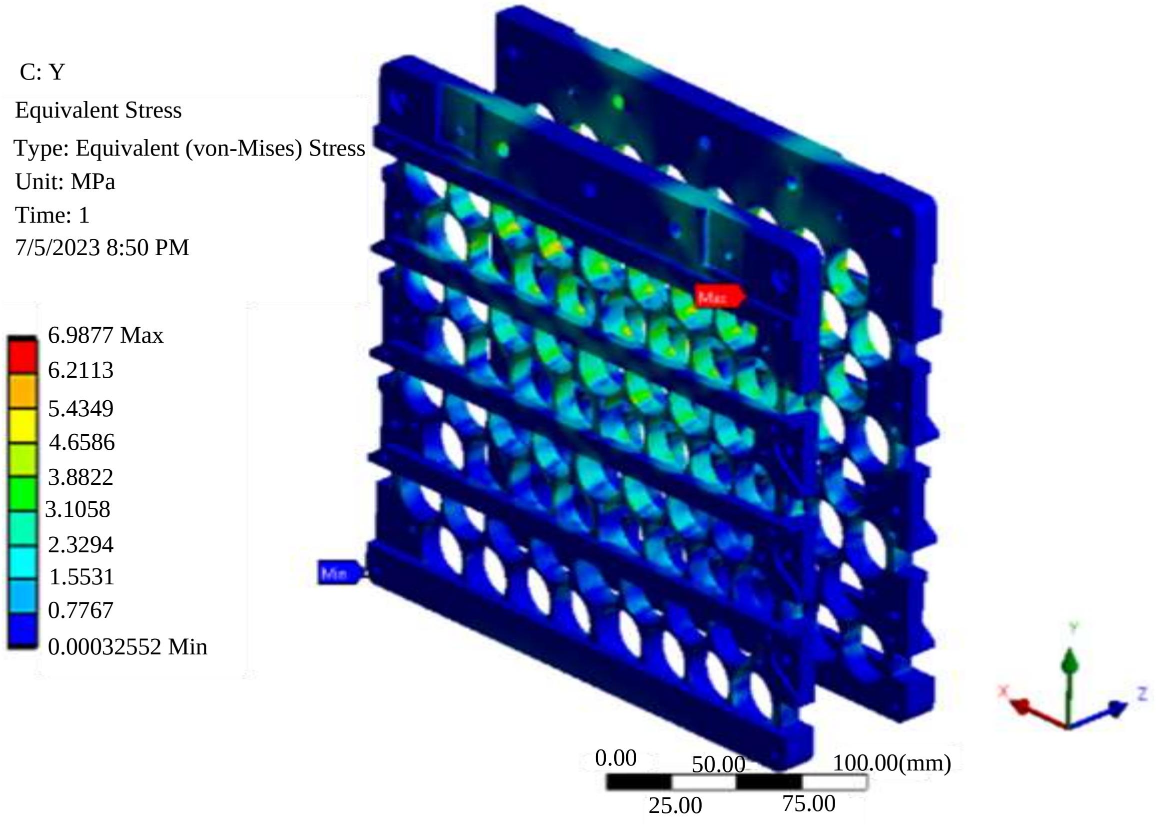

Figure 17. Equivalent Stress of the frames when 20g is applied in the vertical direction.

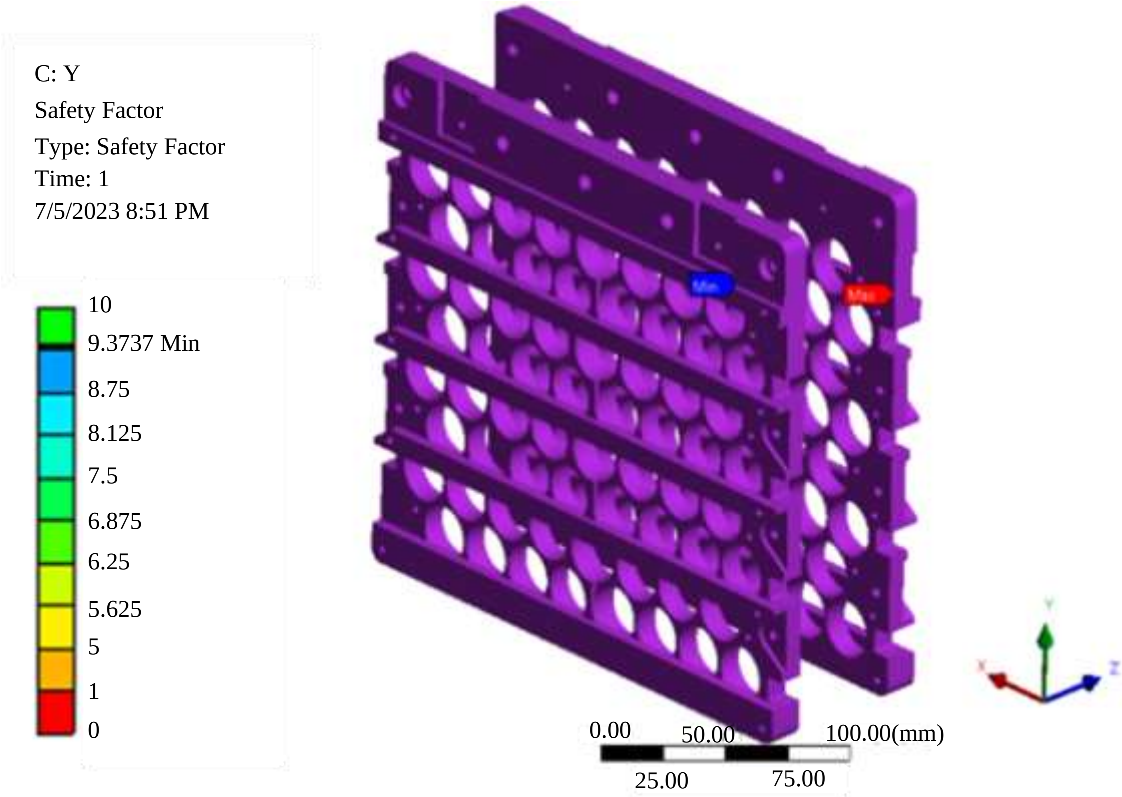

Figure 18. Factor of Safety for the frames when 20kg is applied in the vertical direction.

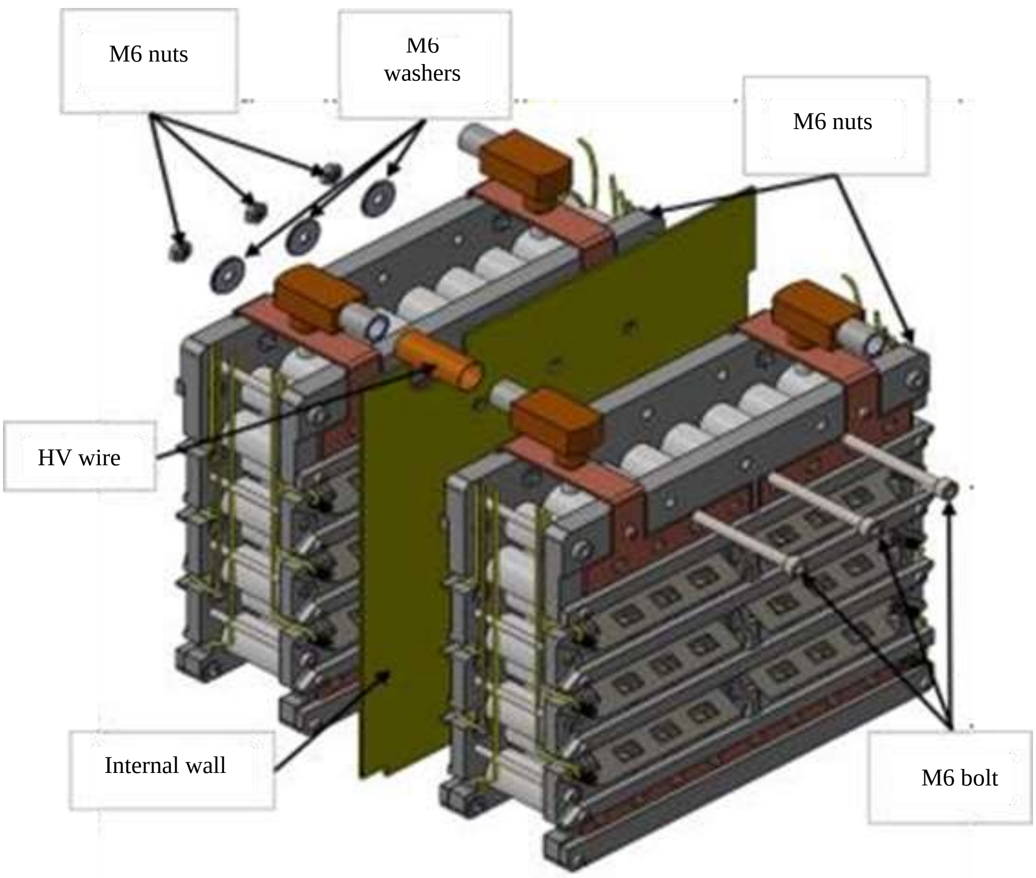

Figure 19. Mounting method of the module to the Tractive System Accumulator Container walls.

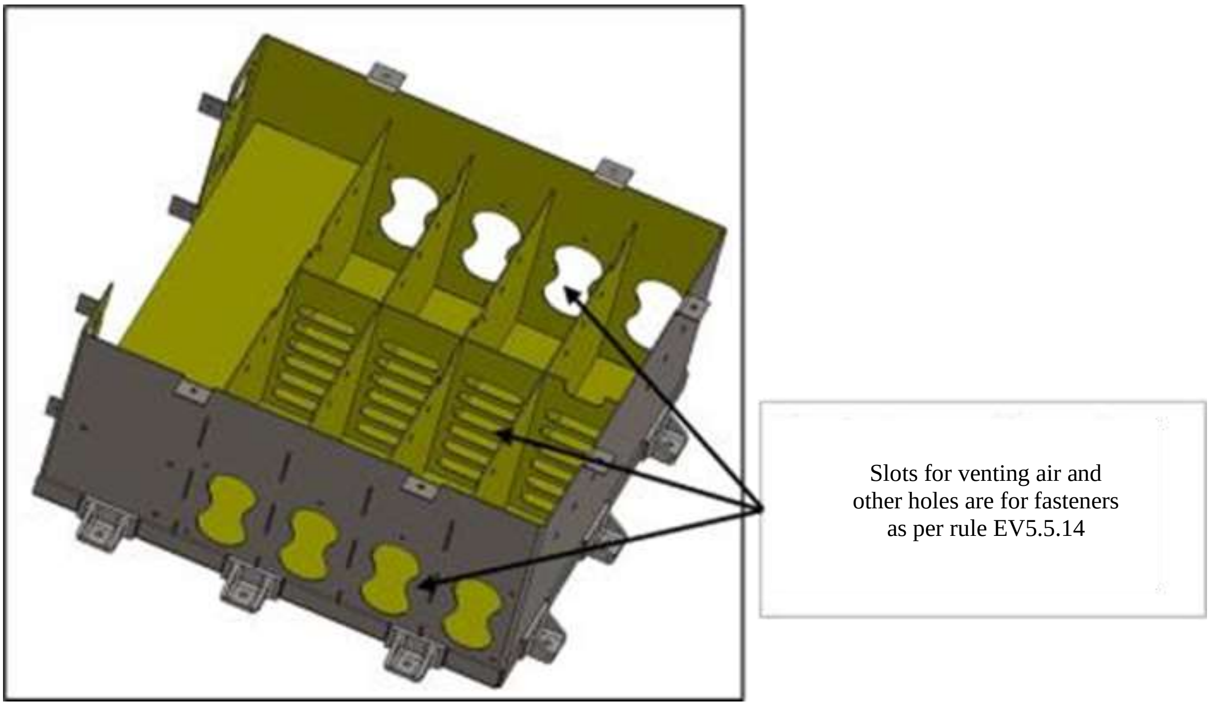

Figure 20. Lateral Vents.

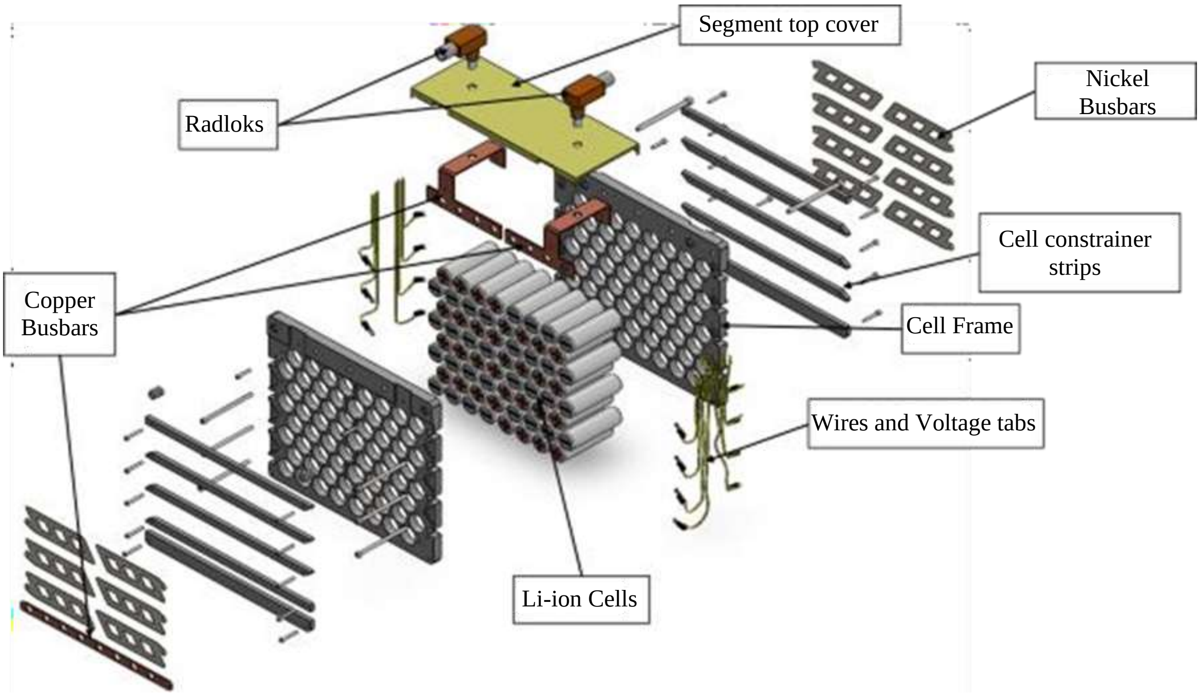

Figure 21. The exploded view of the segment assembly.

THERMAL MANAGEMENT SYSTEM

The accumulator has 21700 lithium-ion cells. The datasheet specifies that the optimal temperature range for the cells to operate effectively is between 0°C and 60°C. A cooling system is required in a battery configuration when the thermal mass of the cells is insufficient to disperse the heat produced by the cells [13,14]. The heat load in this system exceeds the thermal capacity of cells, requiring a thermal management system. Heat in Li-ion cells is primarily due to Joule heating and chemical processes during discharge. Joule heating is the main factor, caused by resistance to electric current flow. High temperatures can lead to decreased performance, accelerated aging, and safety risks [15]. The following calculations were obtained at whose data is later used to imply the boundary conditions for the finite element analysis.

Heat Load: Heat load = Total heat generated - Heat dissipated.

The continuous current rating of accumulator during the endurance run will be limited to 50A. Table 2 lists the parameters under consideration for heat transfer.

Table 2. Heat Transfer Parameters.

Heat Generated		**Dissipated heat used for temperature rise**		**Heat Convected**	
Current Discharge	50A	Cell Mass	0.07 Kg	Cell Diameter	21.7 mm
Internal Resistance	0.016 mOhm	Specific Heat Capacity of cell	1605 J/KgK	Cell Surface Area	0.61 m^2
Endurance Time	2700 Sec	Change in Temperature	30 ˚C	Q (Convected)	10766016 J
Q (Joule Heating)	11197440 J	No. of Cells	128	Convective Heat Transfer Coefficient	217.09 W/m^2K
		Q (Thermal Mass)	431424 J		

Comparative study of different cooling methods

Thermal management is crucial for electric vehicle (EV) battery packs to maintain performance, longevity, and safety. Heat generation during charging can reduce efficiency, shorten lifespan, and increase the risk of thermal runaway. Advanced cooling systems like liquid, air, and phase-change materials are essential to keep the battery within optimal temperature ranges for safe and efficient operation, maximizing battery life and performance in electric vehicles.

Air Cooling

In Battery Thermal Management Systems utilizing air cooling, air is the main source of cooling. The heat generated by the battery dissipates into the air and the battery is cooled. Surface design plays a major role in dissipating the amount of heat [16].

Liquid Cooling

It is a cooling mechanism where a liquid is circulated through battery packs to control the temperature of the battery system. The battery can be cooled by having the liquid directly encounter the battery cell or by having the liquid indirectly interact with the battery cells [16].

Phase Change Material (PCM) Cooling

In this method, a cooling material absorbs heat from the battery by changing from liquid to vapor phase using the latent heat principle. PCM cooling is usually combined with another system for improved efficiency [16].

Forced Convective Air Cooling

For the accumulator, forced convective air cooling was found to be the most effective method. CFD simulation was performed using ANSYS Fluent Software to analyze the staggered arrangement of the cells [17]. Certain considerations were made during this study, which are as follows:

Operating parameters mainly include ambient temperature, air mass flow rate, and battery load. If the ambient temperature exceeds 45◦C, active air cooling can meet the cooling requirements. The Reynolds number of inlet wind speed of the air cooling is usually greater than 3000, so the airflow in the

Accumulator is turbulent. Average Navier-Stokes Equations, and the k - ε turbulence model is used to calculate the turbulence flow [15,16]. The air-cooling Battery Thermal Management System uses 16 fans to cool the whole accumulator as shown in Figure 22. It relies on data fetched by the BMS from the cells, and the open system is waterproofed using a hydrophobic mesh screen to maintain compliance with the competition rules and to prevent water seepage [1, 17].

Fan CFM Calculations

Considering the volume, pressure drop, and heat load, a suitable CFM was selected for a pair of fans (one push and the other pull) to necessitate cooling of 2 inline segments. The geometry of those segments was also considered. Table 3. Gives the hand-calculated values after which an optimal CFM value was obtained. Table 4. States the values of air properties considered for the study. Table 5 enlists the pressure drop values used for calculation and boundary conditions whereas Table 6 gives the results of that calculation.

Table 3. CFM Calculation.

Segment Height	0.19m
Segment Width	0.05m
Cell Diameter	21.7mm
Transverse Pitch	41.57mm
Longitudinal Pitch	12mm
Transverse Pitch Ratio	1.92
Longitudinal Pitch Ratio	0.55
Streamed Length	0.034m
Bundle Nusselt Number	285.78
Arrangement Factor	2.28
No. of Rows	32
Nusselt Number	127.74
Void Factor	0.26
Reynolds Number	21025
Inlet Air Velocity	2.57 m/s
Inlet Area	0.0095m^2
Volumetric Flow Rate	51.74 cfm
1 Fan	25.87cfm

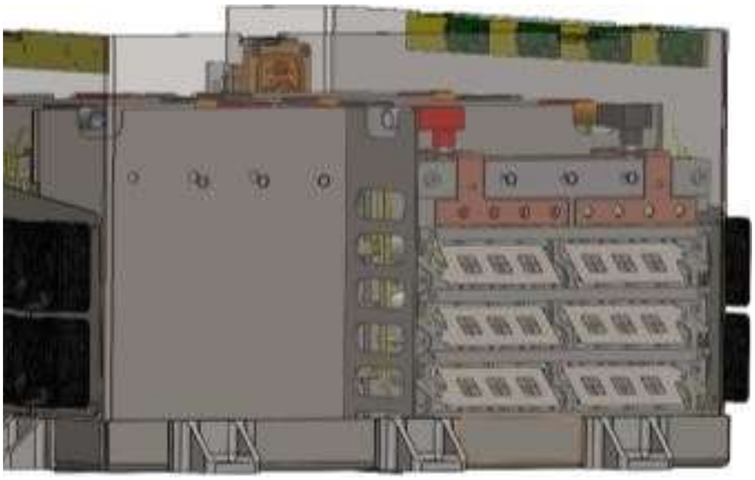

Figure 22. Lateral airflow cooling provision inside the accumulator.

Table 4. Air Properties.

Density	1.164 Kg/m^3
Dynamic Viscosity	0.0000187 Kg/ms
Thermal Conductivity	0.026 W/mK
Prandtl Number	0.728
Specific heat capacity	1007 J/KgK

Table 5. Values used for Pressure drop Calculation.

Sd	0.024m
Flow Velocity	1.5m/s
Number of Rows	32
S1/d	1.92
S2/d	0.55
C	1.22
RHS	1.09902

Table 6. Resultant Values of Pressure Drop Calculation.

If S2/d<RHS		**If S2/d>=RHS**	
Nmr	31	**Nmr**	32
We	6.44 m/s	**We**	3.14 m/s
Re1	8684.21	**Re1**	4234.29
Fv	0.18	**Fv**	0.99
Cr	1.11		
Falv	526.50	**Falv**	218.62
Fatv	3.33	**Fatv**	3.33
Zeta Laminar	0.06	**Zeta Laminar**	0.05
Zeta Turbulent	0.34	**Zeta Turbulent**	0.41
Zeta	0.12	**Zeta**	0.46
Pressure Change	92.00 Pa	**Pressure Change**	84.21 Pa
	0.37 in H_2O		0.34 in H_2O
For 1 Fan	0.18 in H_2O	**For 1 Fan**	0.17 in H_2O

Fan curve and operating point

Since the operating parameters of CFM and pressure drop were obtained, the fan curve from Figure 23 was used to finalize the fan model as stated in Table 7.

Table 7. Selected Fan Model

Model	**CFM at 0.15 Pressure**	**Current**	**Thickness**	**Square Dimension**
MG60151V1-10000-A99	15	0.13	25mm	60mm

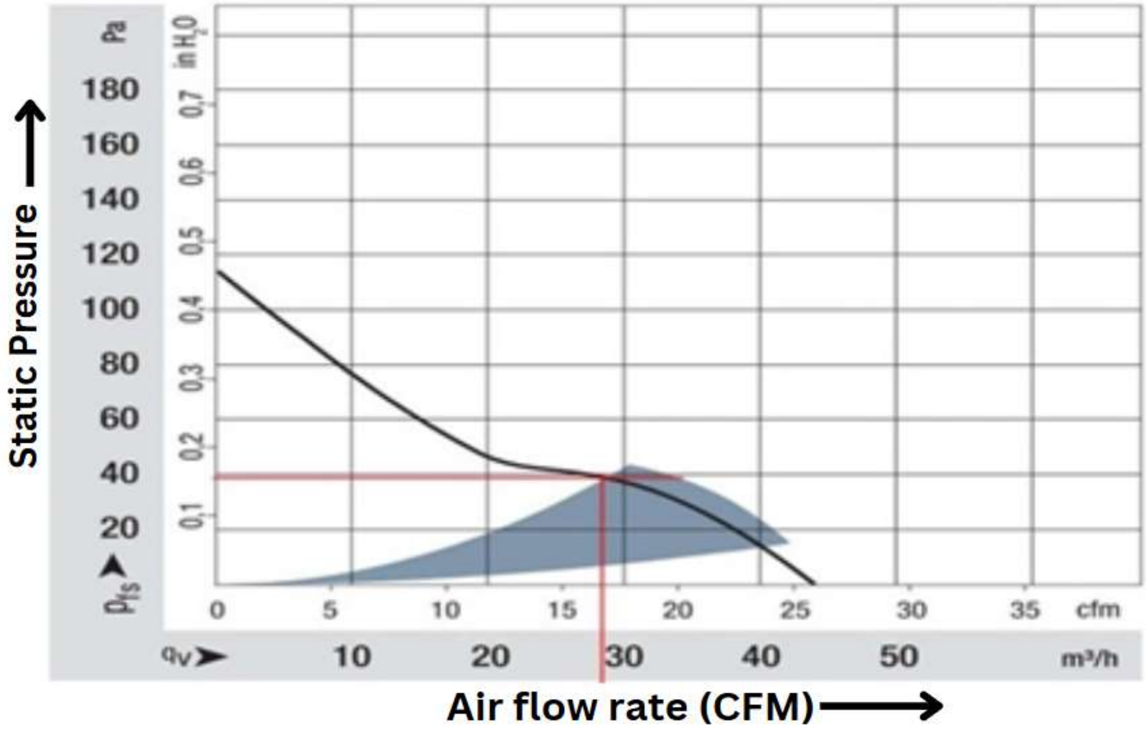

Figure 23. Fan curve.

CFD ANALYSIS

The forced cooling system regulates the temperature of the accumulator. Thermal analysis using the k - ε turbulence model and the Finite Volume Method with meshing is conducted. Boundary conditions are predetermined based on Table 1's datasheet. This model calculates turbulent kinetic energy and dissipation rate to simulate turbulence effects and provides system temperature for set conditions.

Analysis Methodology

FLUENT is a widely recognized software used for modeling and simulating fluid flow and heat transfer problems to solve fluid dynamics equations and generate necessary solutions. Mesh generation plays a crucial role.

For mesh creation in ANSYS FLUENT, both global and local meshing techniques were employed. Since the cell surfaces are cylindrical, the Advanced Sizing function is set to "proximity and curvature" in the global mesh settings [18,19]. The governing equations for the air-cooling pack were solved numerically using the finite volume-based ANSYS

Fluent solver, with the K-epsilon (k-ε) turbulence model and the RNG method applied in this simulation. [16,20]. The analysis was carried out in the following steps:

1. ***3D Modelling:*** SolidWorks was utilized to create 3D models of the cells, exported as an IGS file.
2. ***CFD Analysis:*** ANSYS Fluent software conducted a steady-state analysis.
3. ***Geometry:*** Cells, modelled as staggered solid cylinders, and fluid regions were created in Ansys Design Modeler.
4. ***Meshing:*** An extremely fine mesh would give the best results but the computational time increases drastically. Compromising on mesh size means compromising on accuracy. So, mesh size was selected to give sufficiently accurate results. The mesh size chosen was 2mm. The named selection was created and the inlet, outlet, walls and fluid region were named.
5. ***Setup:*** The analysis was carried out on a single segment. All the properties for a single segment were taken from calculations performed previously. Firstly, the energy equation was turned on.

Keeping in mind the accuracy and computational load we proceeded with the k-epsilon turbulence model. Cells were assigned the suitable properties of thermal conductivity = 3 W/m K, specific heat 1605 J/kg K, mass = 70 grams. [21]

6. ***Boundary Conditions:*** Inlet velocity was set at 1.3382 m/s and outlet pressure at 0 Pa. The calculation was initialized and solved.
7. ***Results:*** The temperature results were well below 60 degrees Celsius and hence the fan values were finalized. Figures 24, 25, and 26 are the snapshots of the temperature distribution analysis.

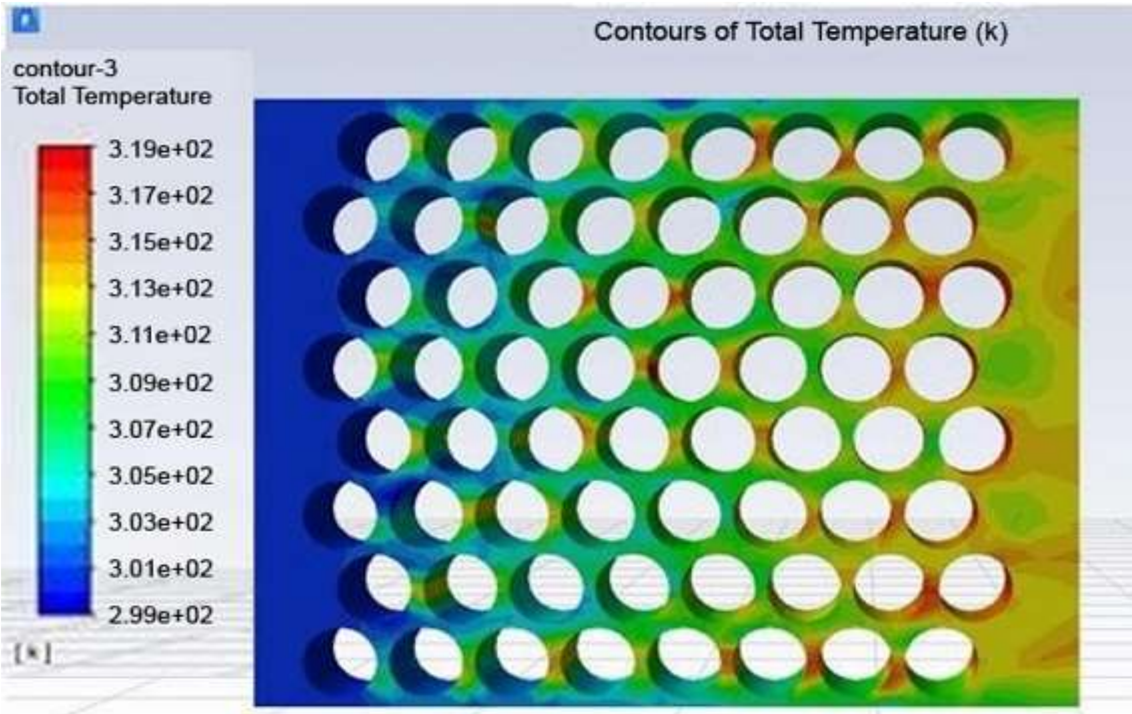

Figure 24. Temperature contours for staggered cell arrangement.

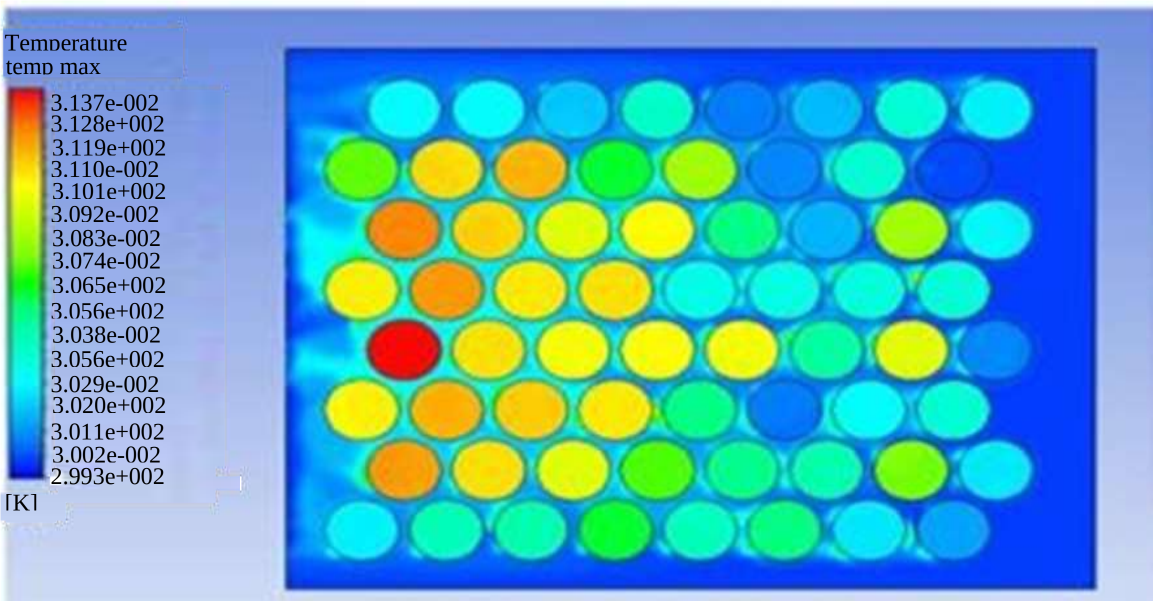

Figure 25. Effect of heating of a single cell on its surrounding cells.

Journal of Polymer & Composites
Volume 13, Special Issue 5
ISSN: 2321-2810 (Online), ISSN: 2321-8525 (Print)

The employed cooling system effectively keeps the operating temperature well below specified limits, ensuring the battery pack is thermally optimal and ready to use, despite Joule Heating and staggered cell arrangement. The airflow within the accumulator is managed and thermal efficiency is around 65%.

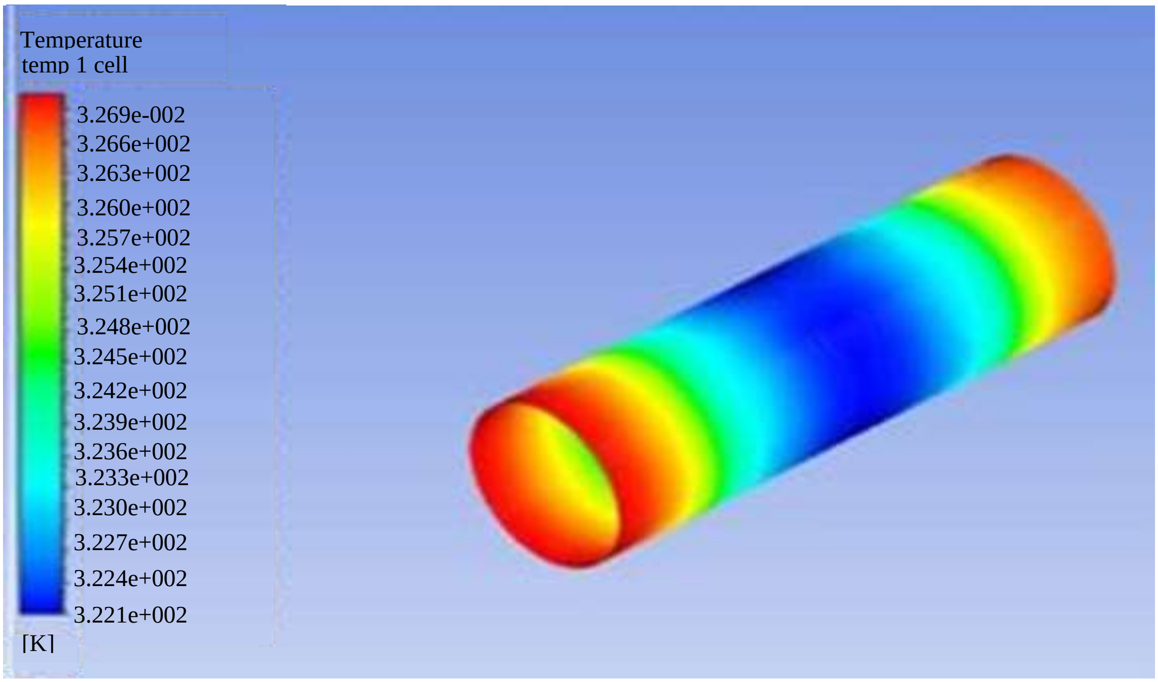

Figure 26. Effect of heating of terminals on the cell body.

CONCLUSION

The results obtained from the thermal analysis performed on FEA software (ANSYS Fluent) indicate that the temperature successfully remained well below the critical threshold of 60°C, affirming the efficacy of the chosen cooling system, i.e., installation of 2X24 CFM fans. With the staggered cell arrangement, heat transfer was optimized, ensuring better overall efficiency and preventing equipment failure. This further confirmed that air cooling using fans would be a viable option. The structural analysis performed on FEA Software (ANSYS Mechanical) proves that the polycarbonate material can withstand the loads with a minimum safety factor of 2.138. This substantial safety factor indicates a significant margin between operational stresses and the failure point, ensuring the design's durability and safety under real-world conditions. These results affirm that the structural design of the battery pack is sound, capable of maintaining its integrity during vehicle operation, and does not require any modifications. Thus, the battery pack is deemed structurally ready for deployment, ensuring confidence in its performance and longevity, implying using advanced material composites for battery pack construction.

The results guide the design process, ensuring that the battery pack maintains optimal operating conditions for performance. The analysis evaluated various loading scenarios, including mechanical stresses and vibrations, verifying that the selected materials and configuration for the battery pack are both robust and resilient. Thus, it is concluded that the accumulator stays well within the threshold temperature, can bear the applicable loads and is operation- ready. This may form the basis of an interesting application for using polymer composites (specifically polycarbonates) in battery pack construction – ensuring both electrical and thermal safety being an insulator.

REFERENCES

1. Formula Student Germany. Rules & Documents [Internet]. 2024 [Cited 2024 Feb 20].

2. Company Resource:https://www.molicel.com/wp-content/uploads/FSSF00058BF-Molicel-RechargeableLithium-ion-cells-and-multi-cell-battery-packs.pdf
3. Sivakumar A, Mohanty P. Electronic System Design of a Formula Student Electric Car. In2020 IEEE International Conference on Distributed Computing, VLSI, Electrical Circuits and Robotics (DISCOVER) 2020 Oct 30 (pp. 115-120). IEEE..
4. Zwicker MF, Moghadam M, Zhang W, Nielsen CV. Automotive battery pack manufacturing–a review of battery to tab joining. Journal of Advanced Joining Processes. 2020 Mar 1;1:100017.
5. Thomsen M, Huang X, Fernandez-Pello C, Urban DL, Ruff GA. Concurrent flame spread over externally heated Nomex under mixed convection flow. Proceedings of the Combustion Institute. 2019 Jan 1;37(3):3801-8.
6. Elenchezhian MR, Nisha Felcy J, Yogeshwari R, Thooyavan M, Madhan Kumar A. Structural Analysis of Lexan Polycarbonate. International Journal of Technology Enhancements and Emerging Engineering research (IJTEEE). 2015.
7. Hareesh K, Pandey AK, Sangappa Y, Bhat R, Venkataraman A, Sanjeev G. Changes in the properties of Lexan polycarbonate by UV irradiation. Nuclear Instruments and Methods in Physics Research Section B: Beam Interactions with Materials and Atoms. 2013 Jan 15;295:61-8.
8. Persic A, Premec A, Magas L, Vrazic M. Battery Package Fused Bus Bar Design for Cylindrical Battery Cells. In2022 26th International Conference Electronics 2022 Jun 13 (pp. 1-6). IEEE.
9. Company Resource - https://ff.sabic.eu/uploads/resources/1607412772-17530460-LEXAN- 9034-9030XXXDATASHEET-US-2020.pdf
10. Madenci, Erdogan, and Ibrahim Guven. The finite element method and applications in engineering using ANSYS®. *Springer*, 2015.
11. Weber S, Montero J, Bleckmann M, Paetzold K. A comparison of layered tetrahedral and cartesian meshing in additive manufacturing simulation. Procedia CIRP. 2020 Jan 1;91:522-7.
12. Basloom HS. A Comparison Study between Tetrahedral Mesh and Hexahedral Mesh. In2018 21st Saudi Computer Society National Computer Conference (NCC) 2018 Apr 25 (pp. 1-6). IEEE.
13. Saw LH, Ye Y, Tay AA. Integration issues of lithium-ion battery into electric vehicles battery pack. Journal of Cleaner Production. 2016 Feb 1;113:1032-45.
14. Verma SP, Saraswati S. Numerical and experimental analysis of air-cooled Lithium-ion battery pack for the evaluation of the thermal performance enhancement. Journal of Energy Storage. 2023 Dec 10;73:108983.
15. Yang R, Wang M, Xi H. Thermal investigation and forced air-cooling strategy of battery thermal management system considering temperature non-uniformity of battery pack. Applied Thermal Engineering. 2023 Jan 25;219:119566.
16. Chen D, Jiang J, Kim GH, Yang C, Pesaran A. Comparison of different cooling methods for lithium ion battery cells. Applied thermal engineering. 2016 Feb 5;94:846-54.
17. Hasan HA, Togun H, Mohammed HI, Abed AM, Homod RZ. CFD simulation of effect spacing between lithium-ion batteries by using flow air inside the cooling pack. Journal of Energy Storage. 2023 Nov 30;72:108631.
18. Zhang SB, He X, Long NC, Shen YJ, Gao Q. Improving the air-cooling performance for lithium-ion battery packs by changing the air flow pattern. Applied Thermal Engineering. 2023 Feb 25;221:119825.
19. Verma SP, Saraswati S. Numerical and experimental analysis of air-cooled Lithium-ion battery pack for the evaluation of the thermal performance enhancement. Journal of Energy Storage. 2023 Dec 10;73:108983.
20. Pelz U, Karlovšek J. Spray-applied waterproofing membranes in tunnelling: A construction perspective. Tunnelling and Underground Space Technology. 2023 Dec 1;142:105409.
21. Hasan HA, Togun H, Abed AM, Biswas N, Mohammed HI. Thermal performance assessment for an array of cylindrical Lithium-Ion battery cells using an Air-Cooling system. Applied Energy. 2023 Sep 15;346:121354.

